Temperature dependence of the electric-field gradient in hcp-Cd from first principles

D. Torumba,[1] K. Parlinski,[2] M. Rots,[1] and S. Cottenier[1,*]
[1]*Instituut voor Kern- en Stralingsfysica–INPAC, Katholieke Universiteit Leuven, Celestijnenlaan 200 D, B-3001 Leuven, Belgium*
[2]*Institute of Technics, Pedagogical University, ulica Podchorążych 2, 30-084 Cracow, Poland*
(Received 5 July 2006; published 13 October 2006)

We determine the temperature dependence of the electric-field gradient in hcp-Cd from first principles. The calculations are based on the *ab initio* determination of the phonon density of states spectrum of the solid. Using only moderate accuracy requirements, the temperature dependence of the electric-field gradient in hcp-Cd is reasonably well reproduced. The origin of its peculiar $T^{3/2}$ dependence is discussed.

DOI: 10.1103/PhysRevB.74.144304 PACS number(s): 63.20.Dj, 71.15.Mb, 71.15.Pd, 76.80.+y

I. INTRODUCTION

Electric-field gradients (EFG) in metals can be calculated nowadays with high precision from first principles. This is an achievement of all-electron implementations of density functional theory, realized during the decade 1985–1995 (Refs. 1–6). Having such a tool, there was no need anymore for the phenomenological equation[7] to describe field gradients that was extensively used during the preceding decades:

$$V_{zz} = (1 - \gamma_\infty)V_{zz}^{latt} + (1 - R)V_{zz}^{el}. \quad (1)$$

It separates contributions to the main component V_{zz} of the field gradient tensor into a remote lattice and a local electron contribution, both modified by often large (anti)shielding factors (R and γ_∞) obtained from model calculations. Analysis of *ab initio* calculated EFG's revealed[2,4,8] a very different picture: the lattice contribution is responsible for the symmetry only and virtually the entire value of the EFG is determined by the valence charge density very close to the nucleus. All this concerns the *magnitude* of V_{zz}. Apart from this magnitude, another experimentally well-documented feature of electric-field gradients in metals is the *temperature dependence* of V_{zz}. Actually, this temperature dependence is surprisingly simple and is reproduced in almost all cases by the following relation:

$$V_{zz}(T) = V_{zz}(0)(1 - BT^\alpha). \quad (2)$$

B is a positive constant in the range 10^{-4} to 10^{-5} $K^{-3/2}$ (i.e., V_{zz} becomes smaller with increasing T) and α is 3/2 over a considerable part of the temperature range in many of the studied cases,[9,10] especially for *sp*-metals. The prototype case of the EFG at ^{111}Cd in hcp-Cd belongs to this class (Fig. 1). For transition metals, smaller values of α can occur, and a fit with Eq. (2) is not always possible. This is illustrated for ^{111}Cd in Zr in Fig. 1. For rare earth[11–16] and actinide[17,18] systems, α=1 is frequently found (Fig. 1). Also when the probe atom does not occupy well-defined lattice positions, anomalous values of α can occur.[19] Especially the occurrence of this peculiar value of 3/2 has triggered a lot of theoretical investigations,[10,20–24] concentrated in the period 1975–1980 and immediately following the experimental observation of this relation (similar methods were applied twenty years before to ionic crystals[25,26]). It was immediately pointed out that the temperature dependence of the lattice constant had only a marginal effect on the EFG and therefore cannot be responsible for this behavior.[27–29] Consequently, all attempts focussed on the next possibility: combining phonon models with Eq. (1).[20–24] As we understand now, Eq. (1) was a flawed starting point, but nevertheless these studies all found that within the framework of Eq. (2) phonons do lead to a temperature dependence that is well-approximated by $T^{3/2}$. Apart from the incorrect Eq. (1), this conclusion suffers additionally from many other approximations used, such as the simple Debye model to describe phonons. As a result, giving a sound theoretical justification for the temperature dependence of the EFG tensor has been identified as one of the open questions in the hyperfine interactions research.[30] In the present paper, we examine the temperature dependence of the EFG of Cd in hcp-Cd (an experimentally very well characterized case[9]) and this fully within an *ab initio* context: EFG's as well as phonons will be calculated from first principles. To our knowledge, this is the first materials-specific theoretical assessment of the temperature dependence of the EFG in a metal that does not rely on empirical or tuneable parameters.

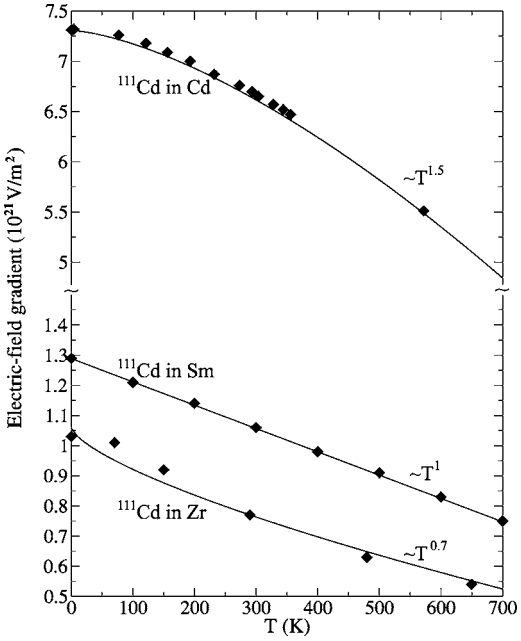

FIG. 1. Different temperature dependence of EFG. Diamonds: experimental data points (Refs. 9, 10, and 15). Solid lines: fit through the experimental values, using the relation $V_{zz}(T) = V_{zz}(0)(1-BT^\alpha)$.

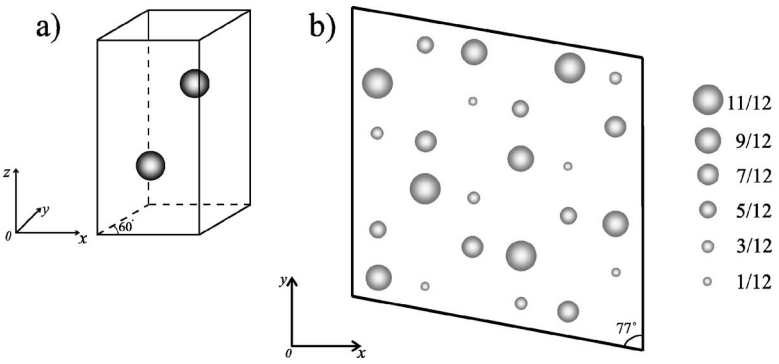

FIG. 2. (a) The unit cell of hcp-Cd used in molecular dynamics calculations. (b) The $2\times2\times1$ rhombohedral supercell (24 atoms), representing the hexagonal structure used in the calculation of the dispersion curves. The atom positions along the z axis are indicated in fractional coordinates ($a=b=c=15.78$ a.u., $\alpha=\beta=\gamma=77.57°$).

II. CALCULATIONS

A. *Ab initio* molecular dynamics

The most straightforward way to examine this temperature dependence, is to apply *ab initio* molecular dynamics (MD): for a sufficiently large piece of material at a given temperature, the position of all atoms is followed as a function of time and track is kept of their instantaneous EFG. Assuming ergodicity, a time average of this EFG then represents the average EFG at that temperature. Such an approach is appealing because it excludes any arbitrariness in the choice of amplitudes and phases of the phonons (see Secs. II A 2 and II B 2): whatever are the initial deviations and velocities given to the atoms, in the end the system should evolve to a well-defined equilibrium dynamic state. However, it might take an enormous amount of time steps before such equilibrium is reached. This is for a necessarily large (unit) cell of simulated matter (to accommodate not just a few short wave length phonons) and using a possibly not very fast (because all electron) *ab initio* code to calculate the forces used by the molecular dynamics scheme. Moreover, it is not guaranteed that within the time span of the simulation all relevant places of phase space will be sampled (the system can get trapped in a subspace). And even if all those objections could be overcome, the results might be numerically true but not necessarily contribute to real insight. Regarding these obstacles, we did a molecular dynamics simulation only for an unrealistically small unit cell of hcp-Cd [see Fig. 2(a)] that is identical to the chemical unit cell (only Γ phonons are possible)—already this simulation exhausted all available computer resources. It will give us some first insight in the time (!) dependence of the EFG and will serve as a consistency check for our following, more realistic attempt with phonon information obtained by the "direct method."[31]

1. Computational details

The *ab initio* calculations were performed within density functional theory,[32–34] using the augmented plane waves +local orbitals (APW+lo) method[34–36] as implemented in the WIEN2K package[37] to solve the scalar-relativistic Kohn-Sham equations. In the APW+lo method, the wave functions are expanded in spherical harmonics inside nonoverlapping atomic spheres of radius R_{MT} and in plane waves in the remaining space of the unit cell (= the interstitial region). For the Cd atoms a R_{MT} value of 2.0 a.u. was used. The maximum ℓ for the expansion of the wave function in spherical harmonics inside the spheres was $\ell_{\max}=10$. The plane wave expansion of the wave function in the interstitial region was made up to $K_{\max}=6.25/R_{\mathrm{MT}}^{\min}=3.13$ a.u.$^{-1}$ and the charge density was Fourier expanded up to $G_{\max}=14\sqrt{\mathrm{Ry}}$. For the sampling of the irreducible part of the Brillouin zone (IBZ) 4704 k points were taken, which corresponds to a $28\times28\times12$ mesh. As exchange-correlation functional, the generalized gradient approximation (GGA96) (Ref. 38) was used. The lattice constants used in these MD calculations were the ones that minimize the total energy and were obtained by optimizing both the volume and the c/a ratio ($a=5.71$ a.u., $c=10.90$ a.u.). We used molecular dynamics with a Nosé thermostat as implemented in the WIEN2K code and this at two temperatures: 50 K and 400 K. The frequency of the thermostat was set at 15 THz and the MD time step was 600 a.u. ($\simeq14.5$ fs).

2. Results

The two atoms in the hcp-Cd unit cell were initially randomly displaced from their equilibrium positions (but conserving inversion symmetry) and the system was let to evolve towards its equilibrium for 11 ps (772 steps, 50 K) or 8 ps (533 steps, 400 K). As it can be seen from Fig. 3 the system oscillates first and reaches near the end of the simulation a thermal equilibrium. The oscillations at equilibrium correspond to Γ phonons. The phonon frequency at the gamma point that corresponds to the vibration in the x and y direction is $\omega_x(\Gamma)=\omega_y(\Gamma)=0.85$ THz, while the vibration along the z axis has a frequency of $\omega_z(\Gamma)=3.13$ THz. In Fig. 3(c) we can also see that the vibrational amplitude at equilibrium depends on temperature ($Q_z^{50\ \mathrm{K}}=0.017$ a.u. and $Q_z^{400\ \mathrm{K}}=0.092$ a.u). The evolution in time of the EFG tensor components can be observed in Fig. 4. V_{xy}, V_{xz}, and V_{yz} are small and go toward zero close to equilibrium, while V_{xx} and V_{zz} oscillate around a nonzero value. As can be observed from Fig. 4(a) (inset), more than 4 ps (277 steps) are needed to get a reasonable equilibrium at a temperature of 400 K. At 50 K an even longer time is needed. In the case of such a small unit cell, the influence of temperature on the EFG turns out to be very small [see Fig. 6(a)]. This can also be observed in Fig. 4(a) where V_{zz} at 50 K and 400 K oscillates (with different amplitudes) around an almost identical mean value. For the highest temperature, this mean value is just barely smaller than for the lowest temperature. In order to see a realistic temperature dependence of the EFG, one

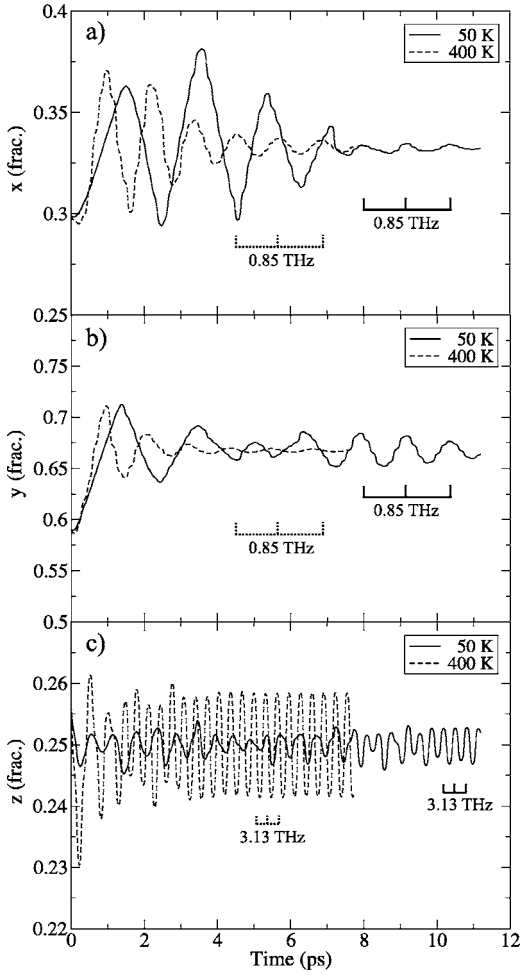

FIG. 3. Atom positions, in fractional coordinates, as a function of time at 50 K and 400 K (772 time steps were calculated for 50 K and 533 time steps for 400 K).

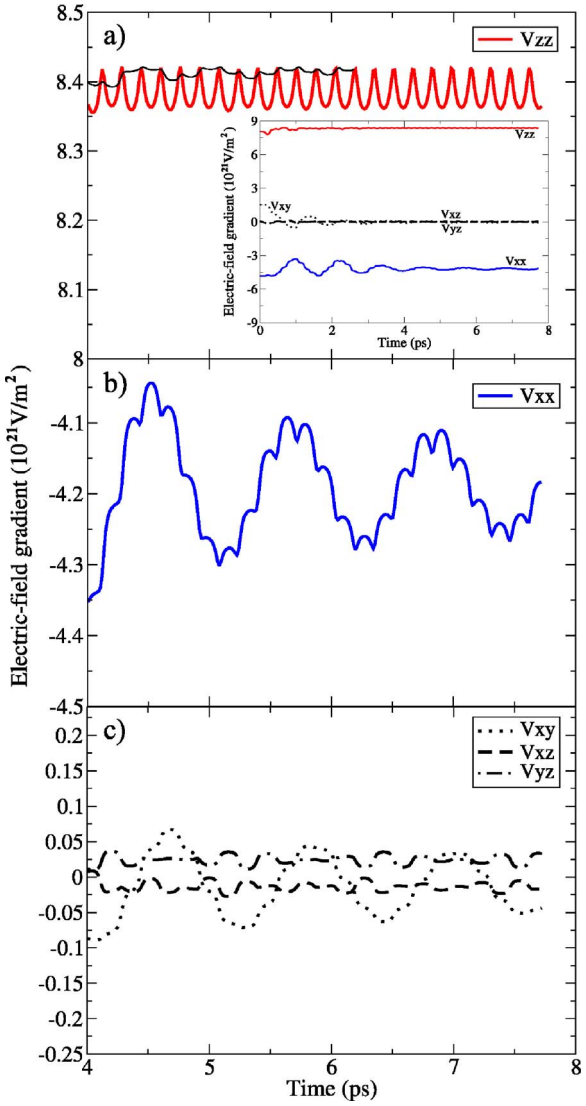

FIG. 4. (Color online) The five components of the EFG tensor close to the equilibrium in the MD simulation at 400 K (the first 4 ps of Fig. 3 are not shown): (a) V_{zz}; (b) V_{xx}; (c) V_{xy}, V_{xz}, and V_{yz}. Inset picture: the complete evolution in time of the five EFG tensor components at 400 K. In (a) V_{zz} at 50 K (the point at 9 ps in Fig. 3 is shifted to coincide with 4 ps in this picture) is also shown (thin black line).

should use a much larger supercell, which is prohibited by computer speed. We now turn to a different approach that will allow one to include more phonons and we will use the MD information as a benchmark.

B. Temperature dependence from phonon dispersion curves

Our second approach is based on the *ab initio* calculation of the phonon dispersion curves. The dispersion relations for hcp-Cd were calculated using the direct method as implemented in the PHONON program,[40] within the harmonic approximation.

1. Computational details

In calculating the phonon dispersion curves for hcp-Cd we have used a $2\times2\times1$ rhombohedral supercell containing 24 atoms [Fig. 2(b)]. The use of this supercell does not reduce the space group symmetry, it only increases the number of atoms by a factor of three compared to the hexagonal $2\times2\times1$ supercell. Then one Cd atom was displaced in several directions and for each displacement the force on this atom and on all other atoms in the cell was *ab initio* calculated (WIEN2K).[37] Technical parameters are: $R_{\mathrm{MT}}=2.5$ a.u. (larger spheres could be taken because now the atoms do not oscillate and can never become very close), $K_{\max}=8.0/R_{\mathrm{MT}}^{\min}=3.2$ a.u.$^{-1}$ (a larger basis set could be afforded compared to MD due to a smaller number of calculations) and a k mesh of 365 points in the IBZ of the large cell ($9\times9\times9$ mesh). Knowing all these forces, the dynamical matrix can be constructed and the phonon dispersion curves (Fig. 5) and polarization vectors of all phonons can be found using the PHONON software.

2. Results

The calculated dispersion curves agree quite well with the experimental ones, obtained from inelastic neutron scattering

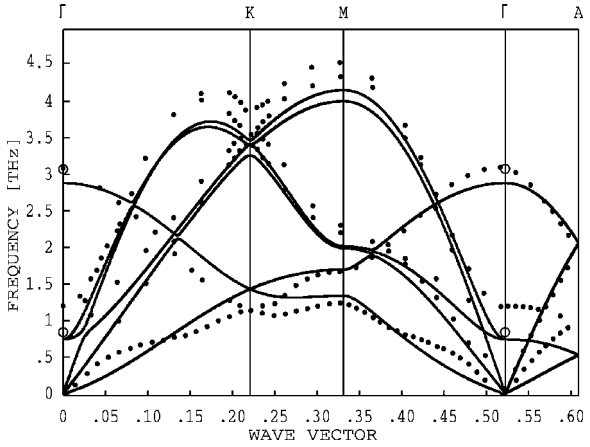

FIG. 5. *Ab initio* calculated phonon dispersion curves for hcp-Cd (solid line) compared with experiment (dots). The frequencies at Γ obtained from MD are indicated by the large open circles.

experiments at 80 K (Ref. 39) (Fig. 5). At Γ there is good agreement with the molecular dynamics results as well (see also Table I). The most obvious difference with experiment is that the calculated optical mode frequencies deviate by about 0.5 THz. Another difference is the shape of the acoustic modes, especially of the transverse acoustical branch. The main reasons for these differences could be, on one hand, the fact that our supercell is still not large enough to confine the interaction range (a prerequisite of the direct method) and, on the other hand, the absence of anharmonic effects. The amplitudes of vibration along the z axis corresponding to the highest optical mode at Γ (at 50 and 400 K) are rather close to the values obtained in the MD simulations [Fig. 3(c)], the difference probably being due to the fact that in our classical MD zero-point vibrations are not included.

The temperature dependence of the electric-field gradient coefficients can be calculated in the following way: in the $2\times2\times1$ cell we displace the atoms according to a set of phonons characterized by the wave vectors commensurate with the cell size and amplitudes, which are described by the average value of the mean square displacements for a given temperature. The displacement amplitudes are similar to those that define the Debye-Waller factor. The property of random phonon phase distribution allows one to choose the phases of phonons randomly (in principle, one should average over all possible random choices—we will do the average only over a finite number of choices, and will verify that that number is large enough). We can now generate a series of configurations in a cell of any size, each configuration having another random choice for the phase. This procedure is equivalent to running simulations over a large time interval, much larger than is possible with *ab initio* MD. Each configuration can subsequently be used as input in an *ab initio* code to calculate the electric-field gradient of any atom, and collect in this way information about the distribution of EFG's over the configurations (i.e., over time).

TABLE I. The phonon frequencies at Γ obtained from MD simulation and from the direct method (DM) compared with experiment (Ref. 39).

	MD		DM			Experiment
T (K)	50	400	0	50	400	80
$\omega_{x,y}$ (THz)	0.85	0.85	0.74	0.74	0.74	1.30
ω_z (THz)	3.13	3.13	2.88	2.88	2.88	3.19

In this approach a limitation to accuracy is that a given cell size can accommodate only a limited set of phonons with wave vectors commensurate to the cell size, to allow for periodic boundary conditions. The larger the cell, the more phonons can be taken into account and the more realistic the approximation. Which cell size should we take? In order to evaluate this we examine the mean square displacements $\langle x^2\rangle$ and $\langle z^2\rangle$ for cells with 24, 56, 1176, and 1920 atoms. They can accommodate 69, 159, 3525, and 5757 phonon modes, respectively. The exact mean square displacements (exact within the harmonic approximation) can be derived from the phonon density of states (DOS). If the cell is sufficiently large, the mean square displacements analytically calculated from all phonons the cell allows, should give the same value. As Table II shows, this is realized only for the largest cell. The quality of the 56-atom cell is no better than the 24-atom cell. Now we take nine random snapshots corresponding to a given temperature and determine $\langle x^2\rangle$ and $\langle z^2\rangle$ for this data set. If the sample of nine is large enough, the values should be identical to the analytical values—Table II shows that taking nine configurations is sufficient for reasonable accuracy. And again the 56-atom cell performs not better than the 24-atom cell. We conclude that a snapshot series from the sequence of a 24-atom cell will produce a rough but qualitatively correct representation of the behavior of the infinite solid and that nothing is gained by moving to 56 atoms. We are interested in small cells because now we will proceed with *ab initio* calculations, which makes large cells unattractive.

For nine different temperatures in the range 0–570 K, nine snapshots of the 24-atom cell were taken. At any given temperature, we observed that the potential energy of a large set of configurations was Gaussian distributed [the potential energy $V=\frac{1}{2}\Sigma_{n,m}\Phi(n,m)U(n)U(m)$, with n and m running over all 24 atomic components, $\Phi(n,m)$ the force constant between atoms n and m, and $U(i)$ the displacement from equilibrium of atom i, measures how "much" a particular configuration is removed from equilibrium]. The nine snapshots were randomly taken out of a much larger set of configurations with this Gaussian distribution as probability density. If this more careful procedure was not followed and a homogeneous probability density was assumed, the average EFG's would differ at most 0.1×10^{21} V/m^2 from the values reported in Fig. 6(a). For each of the $9\times9=81$ selected cases an *ab initio* calculation was done. This was quite demanding, due to the displaced atoms no symmetry was left and therefore the $9\times9\times9$ k mesh yielded 365 points in the IBZ. For all atoms in the unit cell the five components of the EFG were determined in an axis system connected to the crystal. For each temperature this gave $24\times9=216$ EFG's, from which the average was then taken. This average EFG was almost axially symmetric ($\eta\leqslant0.10$) and the z axis of its

TABLE II. Mean square displacements of the Cd atoms obtained by averaging over nine configurations ($\langle\ \rangle_9$), from analytical formula with summation over all wave vectors commensurate with the cell ($\langle\ \rangle_{anl}$) and from the phonon density of states, which give the exact result in the harmonic approximation, ($\langle\ \rangle_{DOS}$).

Supercell		24 atoms ($2\times2\times1$)				56 atoms ($3\times3\times1$)				1176 atoms ($7\times7\times4$)	1920 atoms ($8\times8\times5$)
T (K)		0	280	430	570	0	280	430	570	570	570
$\langle x^2\rangle_9$	(Å^2)	0.0018	0.0142	0.0252	0.0330	0.0020	0.0132	0.0201	0.0266	0.0319	0.0372
$\langle x^2\rangle_{anl}$	(Å^2)	0.0020	0.0136	0.0208	0.0276	0.0021	0.0138	0.0210	0.0279	0.0347	0.0355
$\langle x^2\rangle_{DOS}$	(Å^2)	0.0022	0.0177	0.0273	0.0361	0.0022	0.0177	0.0273	0.0361	0.0361	0.0361
$\langle z^2\rangle_9$	(Å^2)	0.0031	0.0272	0.0422	0.0512	0.0032	0.0289	0.0443	0.0586	0.0901	0.0848
$\langle z^2\rangle_{anl}$	(Å^2)	0.0031	0.0265	0.0406	0.0538	0.0032	0.0300	0.0459	0.0609	0.0794	0.0813
$\langle z^2\rangle_{DOS}$	(Å^2)	0.0035	0.0431	0.0660	0.0875	0.0035	0.0431	0.0660	0.0875	0.0875	0.0875

principal axis system was close ($\leqslant 0.4°$) to the c axis of the crystal, in agreement with the symmetry of the (static) crystal. It was cross checked that taking more snapshots did not significantly alter this average. The V_{zz} component of this average EFG is plotted in Fig. 6(a). As could be expected after the observations made from Table II, the agreement with experiment is not perfect. Nevertheless, the main trend is nicely reproduced. The largest deviations occur at the highest temperature, close to the melting temperature (T_m =594 K). In this region the difference of the mean square displacement between the nine configurations $\langle z^2\rangle_9$, and the exact case $\langle z^2\rangle_{DOS}$ are the largest, and moreover anharmonic effects become important.

All these calculations were done for the same fixed lattice constants, as determined previously at 0 K. In order to examine the influence of the fact that lattice constants increase with temperature, for a few temperatures the set of snapshots was recalculated with lattice constants that were increased by the same factor as experimentally determined.[41] This did not alter the results in a significant way [Fig. 6(a)], in agreement with what was concluded years ago in the framework of Eq. (1).[27–29] A particularly interesting feature of Fig. 6(a) is the EFG determined at 0 K (7.85×10^{21}/m^2), which can be compared with the static *ab initio* value of 7.98×10^{21} V/m^2. The difference of 0.13×10^{21} V/m^2 is quite reliable (see the agreement at 0 K in Table II) and is entirely due to zero-point vibrations. It is not a surprise that this effect is small: if it were large, static *ab initio* EFG's would not have been so close to experiment as they are observed to be. To our knowledge this is the first time a quantitative value for the size of the zero-point vibration effect has been determined for a particular metal.

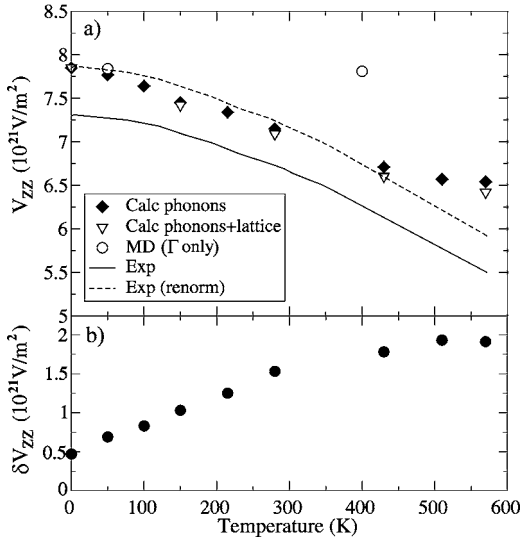

FIG. 6. (a) Calculated values of electric-field gradient for hcp-Cd as a function of temperature: for a fixed lattice constant (diamonds) and for the lattice constant corresponding to that temperature (triangles), compared with experiment. MD results at 50 K and 400 K (circles) are rescaled so that the 50 K result matches the experimental value. (b) The standard deviation of the 9×24 =216 V_{zz} values as a function of temperature.

III. CONCLUSIONS

As a conclusion, we have outlined a procedure to determine from first principles the temperature dependence of the EFG in solids, and tested its feasibility for the prototype case of hcp-Cd. This method is applicable to other quantities than the EFG tensor as well. It can be applied as soon as a quantity does depend on the atom positions only and experimental values are averaged over a time interval that is long compared to the inverse phonon frequencies. If there is a simple relation between this quantity and atomic displacements, then of course this procedure is unnecessarily long, as the *ab initio* step can be skipped. For the case study of the electric-field gradient in hcp-Cd we could not yet carry the method to full accuracy due to limitations in computer power, but nevertheless the experimental trend is rather well reproduced. Better accuracy is expected if larger supercells would be used to determine the phonon dispersion information. Inclusion of anharmonic effects might be needed to get perfect agreement with experiment in the range of highest temperatures. Our results are too rough to make statements about the origin of the $T^{3/2}$ dependence (although the latter's universality should not be overstressed, as Ref. 10 clearly shows). From the point of view of our method, this behavior originates from an average over many phonons, and following Ref. 24 one might wonder whether it is more than a mere accident that in many cases such an average produces a

$T^{3/2}$-like dependence. The astonishing simplicity of Eq. (2), however, still feeds the hope that more precise calculations might find a physical reason for this exponent.

ACKNOWLEDGMENTS

Helpful discussions with P. Blaha (Vienna) are gratefully acknowledged. Work in Leuven was performed in the frame of Projects Nos. G.0239.03 and G.0447.05 of the *Fonds voor Wetenschappelijk Onderzoek-Vlaanderen* (FWO), the Concerted Action Programme of the K. U. Leuven (GOA/2004/02), the Centers of Excellence Programme of the K. U. Leuven (INPAC EF/05/005) and the Inter-University Attraction Pole Programme (IUAP P5/1). The authors are indebted to L. Verwilst, J. Knuts, and P. Mallaerts for their invaluable technical assistance concerning the computer facilities in Leuven.

*Electronic address: Stefaan.Cottenier@fys.kuleuven.be

[1] P. Blaha, K. Schwarz, and P. Herzig, Phys. Rev. Lett. **54**, 1192 (1985).
[2] P. Blaha, K. Schwarz, and P. H. Dederichs, Phys. Rev. B **37**, 2792 (1988).
[3] C. Ambrosch-Draxl, P. Blaha, and K. Schwarz, J. Phys.: Condens. Matter **1**, 4491 (1989).
[4] K. Schwarz, C. Ambrosch-Draxl, and P. Blaha, Phys. Rev. B **42**, 2051 (1990).
[5] P. Dufek, P. Blaha, and K. Schwarz, Phys. Rev. Lett. **75**, 3545 (1995).
[6] H. M. Petrilli, P. E. Blöchl, P. Blaha, and K. Schwarz, Phys. Rev. B **57**, 14690 (1998).
[7] R. E. Watson, A. C. Gossard, and Y. Yaffet, Phys. Rev. **140**, A375 (1965).
[8] S. J. Asadabadi, S. Cottenier, H. Akbarzadeh, R. Saki, and M. Rots, Phys. Rev. B **66**, 195103 (2002).
[9] J. Christiansen, P. Heubes, R. Keitel, W. Klinger, W. Loeffler, W. Sandner, and W. Withhuhn, Z. Phys. B **24**, 177 (1976).
[10] H. C. Verma, Hyperfine Interact. **15/16**, 207 (1983).
[11] M. Forker and W. Steinborn, Phys. Rev. B **20**, 1 (1979).
[12] T. Butz and B. Lindgren, Phys. Scr. **21**, 836 (1980).
[13] R. L. Rasera, B. D. Dunlap, and G. K. Shenoy, Phys. Rev. B **23**, 3560 (1981).
[14] M. Forker, Hyperfine Interact. **24-26**, 907 (1985).
[15] M. Forker and L. Freise, Hyperfine Interact. **34**, 329 (1987).
[16] V. V. Krishnamurthy, S. N. Mishra, S. H. Devare, H. G. Devare, S. Ramakrishnan, V. Srinivas, and G. Chandra, Hyperfine Interact. **80**, 1005 (1993).
[17] U. Hütten, R. Vianden, and E. N. Kaufmann, Hyperfine Interact. **34**, 213 (1987).
[18] S. Cottenier, A. Toye, J. C. Spirlet, J. Winand, and M. Rots, J. Magn. Magn. Mater. **140**, 1263 (1995).
[19] E. N. Kaufmann and R. Vianden, Phys. Rev. Lett. **38**, 1290 (1977).
[20] P. Jena, Phys. Rev. Lett. **36**, 418 (1976).
[21] K. Nishiyama, F. Dimmling, T. Kornrumpf, and D. Riegel, Phys. Rev. Lett. **37**, 357 (1976).
[22] D. R. Torgeson and F. Borsa, Phys. Rev. Lett. **37**, 956 (1976).
[23] M. D. Thompson, P. C. Pattnaik, and T. P. Das, Phys. Rev. B **18**, 5402 (1978).
[24] K. W. Lodge, J. Phys. F: Met. Phys. **9**, 2035 (1979).
[25] H. Bayer, Z. Phys. **130**, 227 (1951).
[26] T. Kushida, G. B. Benedek, and N. Bloembergen, Phys. Rev. **104**, 1364 (1956).
[27] W. W. Simmons and C. P. Slichter, Phys. Rev. **121**, 1580 (1961).
[28] R. S. Raghavan, E. N. Kaufmann, and P. Raghavan, Phys. Rev. Lett. **34**, 1280 (1975).
[29] P. Raghavan, E. N. Kaufmann, R. S. Raghavan, E. J. Ansaldo, and R. A. Naumann, Phys. Rev. B **13**, 2835 (1976).
[30] H. Haas, Hyperfine Interact. **129**, 493 (2000).
[31] K. Parlinski and M. Parlinska-Wojtan, Phys. Rev. B **66**, 064307 (2002).
[32] P. Hohenberg and W. Kohn, Phys. Rev. **136**, B864 (1964).
[33] W. Kohn and L. J. Sham, Phys. Rev. **140**, A1133 (1965).
[34] S. Cottenier, *Density Functional Theory and the Family of (L)APW-Methods: A Step-By-Step Introduction* (Instituut voor Kern-en Stralingsfysica, K. U. Leuven, Belgium, 2002) (to be found at http://www.wien2k. at/reg_user/textbooks).
[35] E. Sjöstedt, L. Nordström, and D. J. Singh, Solid State Commun. **114**, 15 (2000).
[36] G. K. H. Madsen, P. Blaha, K. Schwarz, E. Sjöstedt, and L. Nordström, Phys. Rev. B **64**, 195134 (2001).
[37] P. Blaha, K. Schwarz, G. Madsen, D. Kvasnicka, and J. Luitz, *WIEN2k, An Augmented Plane Wave+Local Orbitals Program for Calculating Crystal Properties* (Karlheinz Schwarz, Technische Universität Wien, Austria, 1999).
[38] J. P. Perdew, K. Burke, and M. Ernzerhof, Phys. Rev. Lett. **77**, 3865 (1996).
[39] B. Dorner, A. A. Chernyshov, V. V. Pushkarev, A. Y. Rumyantsev, and R. Pynn, J. Phys. F: Met. Phys. **11**, 365 (1981).
[40] K. Parlinski, *Software Phonon* (2003).
[41] P. Villars and L. D. Calvert, *Pearson's Handbook of Crystallographic Data for Intermetallic Phases* (ASM International, Materials Park, Ohio, 1985).